

# Growth and evolution of satellites in a Jovian massive disc

R. A. Moraes,<sup>1,2★</sup> W. Kley<sup>2★</sup> and E. Vieira Neto<sup>1★</sup>

<sup>1</sup>UNESP, Univ. Estadual Paulista – Grupo de Dinâmica Orbital & Planetologia, Guaratinguetá, CEP 12.516-410, São Paulo, Brazil

<sup>2</sup>Institut für Astronomie und Astrophysik, Universität Tübingen, Auf der Morgenstelle 10, D-72076 Tübingen, Germany

Accepted 2017 December 13. Received 2017 December 13; in original form 2017 June 29

## ABSTRACT

The formation of satellite systems in circum-planetary discs is considered to be similar to the formation of rocky planets in a proto-planetary disc, especially super-Earths. Thus, it is possible to use systems with large satellites to test formation theories that are also applicable to extrasolar planets. Furthermore, a better understanding of the origin of satellites might yield important information about the environment near the growing planet during the last stages of planet formation. In this work, we investigate the formation and migration of the Jovian satellites through  $N$ -body simulations. We simulated a massive, static, low-viscosity, circum-planetary disc in agreement with the minimum mass sub-nebula model prescriptions for its total mass. In hydrodynamic simulations, we found no signs of gaps, therefore type II migration is not expected. Hence, we used analytic prescriptions for type I migration, eccentricity and inclination damping, and performed  $N$ -body simulations with damping forces added. Detailed parameter studies showed that the number of final satellites is strongly influenced by the initial distribution of embryos, the disc temperature, and the initial gas density profile. For steeper initial density profiles, it is possible to form systems with multiple satellites in resonance while a flatter profile favours the formation of satellites close to the region of the Galilean satellites. We show that the formation of massive satellites such as Ganymede and Callisto can be achieved for hotter discs with an aspect ratio of  $H/r \sim 0.15$  for which the ice line was located around  $30R_J$ .

**Key words:** planets and satellites: formation – planets and satellites: individual: (Galilean satellites).

## 1 INTRODUCTION

Orbiting Jupiter we have the most famous family of regular satellites in our Solar system, the Galilean satellites. These bodies are in almost circular and coplanar orbits, rotating in the same direction as the rotation movement of Jupiter. Such characteristics led to a well-accepted theory that these bodies were formed in a circum-planetary disc around Jupiter (Lunine & Stevenson 1982). This formation scenario somehow resembles the scenario proposed for formation of our Solar system, for such that the Galilean system is often called a ‘mini Solar system’. Studying the formation of this satellite system could provide information about the last stages of formation of Jupiter. Nowadays there are two competitive models that aim to describe the origin of the regular satellites in a circum-planetary disc, the minimum mass sub-nebula (MMSN) model (Lunine & Stevenson 1982; Mosqueira & Estrada 2003a,b; Estrada et al. 2009) and the gas-starved disc model (Canup & Ward 2002, 2006, 2009).

The gas-starved disc model proposes an initially low-mass disc that is continuously supplied by the infall of material from the circum-stellar proto-planetary disc. In this model, the formation of the satellites takes place at the same time as the formation of the parent planet. Kley (1999) and Lubow, Seibert & Artymowicz (1999) showed that after the forming planet opens its gap in the disc, the flow of mass towards the planet is not halted and the planet continues to grow from this material. This continuous inflow of material will provide a source for the satellites to grow, always maintaining a low surface density disc with a peak of  $100 \text{ g cm}^{-2}$ . In this model, the first generation of satellites forms and performs a type I migration through the disc, then a second generation of satellites forms and repeats the same process. In this way, the Galilean satellites were only the last generation of satellites formed in the circum-planetary disc around Jupiter. The low surface density increases the time of formation of the Galilean satellites, using the process of inflow of material to add the amount of mass needed to form massive bodies, this feature corroborates the idea of a late formation of Callisto (the outermost satellite). However, Mosqueira & Estrada (2003b) argued that this mechanism could not only delay the process of satellite formation but also prevent it. The gas-starved disc model

\* E-mail: [ricardo.moraes07@gmail.com](mailto:ricardo.moraes07@gmail.com) (RAM); [wilhelm.kley@uni-tuebingen.de](mailto:wilhelm.kley@uni-tuebingen.de) (WK); [ernesto@feg.unesp.br](mailto:ernesto@feg.unesp.br) (EVN)

**Table 1.** Properties and fraction of rock and ice of the Galileans satellites, where  $a$ ,  $M$ , and  $e$  are the semimajor axis (in units of the radii of Jupiter), the mass (in units of  $10^{-5}$  masses of Jupiter) and the eccentricity of the satellites, respectively.

Satellites	$a$ $R_J$	$M$ $10^{-5}M_J$	$e$	Rock %	Ice %
Io	5.9	4.7	0.0041	100	0
Europa	9.4	2.5	0.01	~82	~8
Ganymede	15.0	7.8	0.0015	~55	~45
Callisto	26.4	5.7	0.007	~44	~56

is widely used by several authors to study the formation of regular satellites in other planets of our Solar system and in extrasolar systems (Heller & Pudritz 2015a,b).

A competitive model for the gas-starved disc model is the MMSN model. This model was first proposed to describe the formation of the planets system in our Solar system (Weidenschilling 1977; Hayashi 1981) and was later adapted for satellite systems. In the MMSN model, a massive disc with a peak surface density around  $10^5 \text{ g cm}^{-2}$  is accumulated by infall of gas through the Lagrangian points of the planet at the late stages of its formation. In this case, the disc is static, with no inflow of material and has a low turbulence during the evolution of the satellites, in Mosqueira & Estrada (2003a), for example, the authors considered an isolated disc where the turbulence does not play a role any more. Up to date, there is no consensus about which model can describe better the formation of satellites and several semi-analytical studies had been performed in order to explore more parameters of both models (Sasaki, Stewart & Ida 2010; Ogihara & Ida 2012; Miguel & Ida 2016).

The properties and characteristics of the Galileans satellites are very peculiar. Starting with their sizes and masses, these satellites are amongst the most massive in our Solar system (Table 1) including Titan and Triton, orbiting Saturn and Neptune, respectively. The largest satellite, Ganymede, is larger than the planet Mercury. The composition of these satellites and their fraction of ice is different, which means that the temperature in the disc during the formation of the satellites was different. The increasing ice fraction per distance in the Galilean system may imply that near the planet the temperature was higher than farther out.

The current dynamical configuration of the Galileans is also interesting. Io, Europa and Ganymede are locked in a 1:2:4 mean motion resonance. In this way, the successive conjunction of these bodies occurs always close to the same longitude. The Galilean satellites are also in the Laplace resonance with resonant angle defined as,

$$\phi = \lambda_I - 3\lambda_E + 2\lambda_G, \quad (1)$$

where  $\lambda_I$ ,  $\lambda_E$ , and  $\lambda_G$  are the mean longitude of Io, Europa and Ganymede, respectively. In the case of these satellites, the resonant angle liberates around  $180^\circ$  ( $\phi \approx 180^\circ$ ). This implies that when Europa and Ganymede are in conjunction (with respect to Jupiter), i.e.  $\lambda_E = \lambda_G$ , Io will be in the opposite position, because  $\lambda_I - \lambda_E = \lambda_I - \lambda_G \approx 180^\circ$ . In this way, a triple conjunction is impossible.

The resonances in the Galilean system is a signature of orbital migration during or after their formation (Ogihara & Ida 2012). In order to explain the resonances using orbital migration, two different theoretical scenarios were proposed. In the first scenario, Yoder (1979) and Yoder & Peale (1981) argued that Io migrates outwards due to the gravitational tides from Jupiter and eventually captured Europa in a 2:1 mean motion resonance, after this point the orbital

expansion continues and Europa encountered Ganymede, forming a new 2:1 commensurability, finally resulting in the Laplace resonance. In the second scenario, Greenberg (1987) and Peale & Lee (2002) associated the resonances with an inward type I migration; in this case, the most massive satellite, Ganymede, performed a rapid type I migration through the disc until capture the inner satellites in the Laplace resonance. The second scenario as it was initially proposed has problems, Canup & Ward (2006) showed through  $N$ -body simulations that when a satellite in the outer disc reaches a mass comparable with Ganymede, the satellites in the inner disc are less massive than Io and Europa. In this way, a possible solution could be the migration of a Ganymede-size satellite after the satellites in the inner region have been already formed.

In this work, we study the scenario of formation of satellite systems with the characteristics of the Galileans under the assumptions of the classical MMSN model. We performed several  $N$ -body simulations using the package MERCURY (Chambers 1999) including type I migration and eccentricity and inclination damping adapted from Cresswell & Nelson (2008) to act on the proto-satellites embryos, and an aero-dynamical drag (Adachi, Hayashi & Nakazawa 1976) that will act over the satellitesimals. Throughout the simulations, we explored different parameters such as the radial distribution and masses of the solids, density profile of the gaseous nebula, and the aspect ratio of the disc.

This paper is organized as follows. In Section 2, we explain the model and show the parameters used. The results of our simulations are presented in Section 3, and in Section 4, we point out our conclusions.

## 2 THE MODEL

According to the MMSN model, the Galilean satellites will form in a circum-planetary disc around Jupiter during the late stages of the formation of the planet. At this point, the gas infall on to Jupiter is already finished and the turbulence in the circum-planetary disc is weak. We will apply these premises to our model as will be described below.

### 2.1 System

We consider a coordinate system centred on the planet without the effects of the Sun. As we are working at the final stages of Jupiter's formation, the circum-planetary disc is immersed in the gap opened by the planet. Unless we state differently, the circum-planetary disc will be composed of gas, satellitesimals, and satellite embryos. Following the MMSN assumptions, the total mass of gas and solids (satellitesimals and embryos) in the disc will be  $M_{\text{gas}} \sim 2 \times 10^{-2} M_J$  and  $M_{\text{solid}} \sim 2 \times 10^{-4} M_J$ , respectively. All the solids in the disc are affected by the presence of the gas, and the embryos will gravitationally interact with each other and with the satellitesimals, while the gravitational interaction between satellitesimals will be neglected.

Because of the uncertainties in the initial solid surface density, we decided to neglect the increase of solid surface density due to ice condensation (Miguel & Ida 2016); also, we choose the gas-to-dust ratio to be equal to 100, analogous to the solar nebula.<sup>1</sup> In Section 3.8, we discuss a model with enhanced amount of solids.

<sup>1</sup> Other gas-to-dust ratios could be tested, usually keeping the total mass of solids in the disc and decreasing the gas surface density. These models are known as solid-enhanced minimum-mass model (Mosqueira & Estrada 2003b; Estrada et al. 2009).

The density profile and the radial distribution will be addressed later, once the characteristics of the solids disc will be different for each simulation.

## 2.2 The disc structure

As pointed out by Miguel & Ida (2016) there are many factors that should be taken into account when we define the gas surface disc distribution for a circum-planetary disc around Jupiter, such as the infall and viscous accretion on to the planet. As we are not interested in developing a very sophisticated model for the Jupiter's nebula, we will argue that when a satellitesimal (or embryo) becomes large enough to decouple from the inflowing gas, the drag forces generated by the gas in the disc will not play an important role when these bodies cross the denser parts of the disc, which would be in the vicinity of the planet. Hydrodynamic simulations had shown that for these locations the gas distribution is approximately axisymmetric (Tanigawa, Ohtsuki & Machida 2012). Thus, we assume the following radial vertical distribution for the gas density of the circum-planetary disc:

$$\rho_{\text{gas}}(r, z) = \frac{\Sigma_{\text{gas}}(r, t)}{\sqrt{\pi}H} \exp\left(-\frac{z^2}{H^2}\right), \quad (2)$$

where  $\Sigma_{\text{gas}}(r, t)$  and  $H$  are the gas surface density and the scale height of the circum-planetary disc, respectively, given by

$$\Sigma_{\text{gas}}(r, t) = \Sigma_{\text{gas},t} \left(\frac{r}{R_0}\right)^{-\beta} \quad (3)$$

and

$$H = 0.05r. \quad (4)$$

The length scale,  $R_0 = 150R_J$ , corresponding to the effective size of the circum-planetary disc,  $\Sigma_{\text{gas},t}$  is given by equation (5), and  $\beta = 3/2$  is the local surface density profile.

For our disc model, we adopted an exponential prescription in time for the gaseous disc dissipation given by Ida & Lin (2004)

$$\Sigma_{\text{gas},t} = \Sigma_{\text{gas},0} \exp\left(-\frac{t}{\tau_{\text{disc}}}\right), \quad (5)$$

where  $t$  is the time,  $\Sigma_{\text{gas},0}$  is the initial density at  $R_0$ , and  $\tau_{\text{disc}}$  is the global disc diffusion time-scale given by

$$\tau_{\text{disc}} \sim 3 \times 10^5 \frac{R_{\text{disc}}}{100R_J} \left(\frac{\alpha}{10^{-5}}\right)^{-1} \text{ yr}. \quad (6)$$

The viscous parameter  $\alpha$  depends of the turbulence in the disc, and as shown by Turner, Lee & Sano (2014), Fujii et al. (2014) and, more recently, Fujii et al. (2017), there is an absence of magnetorotational instability (MRI) active regions in the circum-planetary disc, which suggest a value for  $\alpha$  smaller than  $10^{-3}$ . Here, we adopted  $\alpha$  between  $10^{-4}$  and  $10^{-5}$  (Stoll & Kley 2014), which implies  $\tau_{\text{disc}}$  proportional to values between  $10^4$  and  $10^5$  yr.

In our disc models, we use a given temperature profile for the disc, for which we assume a constant aspect ratio. In the first set of models, we use  $h = 0.05$  (a value often used for the Solar nebula) that results in a temperature profile for the disc given by

$$T = T_0 \left(\frac{r}{R_J}\right)^{-1}, \quad (7)$$

where  $T_0 = 545$  K is the temperature at  $1R_J$ . In a second set of models, we use a higher aspect ratio,  $h = 0.15$ , which places the ice line at about  $30R_J$ , in this case  $T_0 \sim 4902$  K.

## 2.3 Equations of motion

We performed  $N$ -body simulations for our numerical calculations with the package MERCURY (Chambers 1999). In all the simulations, when two bodies collide we consider perfect merging with conservation of angular momentum.

In planetocentric coordinates, the equations of motion of the particle  $k$  at distance  $r_k$  are

$$\frac{d^2 \mathbf{r}_k}{dt^2} = -GM_p \frac{\mathbf{r}_k}{|\mathbf{r}_k|^3} - \sum_{i \neq k} GM_i \frac{\mathbf{r}_k - \mathbf{r}_i}{|\mathbf{r}_k - \mathbf{r}_i|^3} - \sum_i GM_i \frac{\mathbf{r}_i}{|\mathbf{r}_i|^3} + \mathbf{F}_{\text{mig}} + \mathbf{F}_{\text{damp},e} + \mathbf{F}_{\text{damp},l} + \mathbf{F}_{\text{drag}}, \quad (8)$$

where  $k, i = 1, 2, \dots, n$ . The terms on the right-hand side of equation (8) are the gravitational force from the planet (central body), the mutual gravity interaction between the bodies, the indirect terms, the tidal damping in the semimajor axis for the satellites embryos (type I migration), eccentricity damping, inclination damping, and aero-dynamic gas drag over satellitesimals, respectively.

## 2.4 Gas effects

Satellitesimals and embryos interact with the circum-planetary disc differently. The satellitesimals are small and feel only the headwind from the gas, the embryos are massive enough to produce density waves in the disc, and are affected by torques from these waves. We will use different approaches to take into account the gas interaction with the different bodies.

The aero-dynamical drag is responsible for transfer angular momentum from the gas to the satellitesimals. Generally, the gas is rotating with a sub-Keplerian speed and the interaction with the satellitesimals causes these bodies to migrate inwards. In our models, we implemented the aero-dynamical gas drag acceleration given by Adachi et al. (1976),

$$\mathbf{a}_{\text{drag}} = -\frac{3C_d \rho_{\text{gas}} v_{\text{rel}}}{8\rho_{\text{sat}} R_{\text{sat}}} \mathbf{v}_{\text{rel}} \quad (9)$$

with  $C_d$  being the drag coefficient calculated as described by Brasser, Duncan & Levison (2007),  $v_{\text{rel}}$  is velocity of the satellitesimals with respect to the gas,  $\rho_{\text{sat}}$  and  $R_{\text{sat}}$  are the density and the radius of the bodies. The intensity of the drag dramatically depends of the radius of the bodies; in our simulations, we set the radius of all satellitesimals to 10 km.

To reproduce the effects of the gaseous disc on the satellite embryos, we will separate the effects in two categories, considering that the eccentricity and inclinations of the embryos can be different than zero. First, the response of the embryos to the density waves produced by the embryos cause those bodies to exchange angular momentum with the disc and migrate inwards in a type I regime. Secondly, if the embryos are eccentric and/or inclined, the interaction with the disc will damp both eccentricity and inclination, leading to circular and coplanar embryos (Izidoro, Morbidelli & Raymond 2014).

To properly take those effects into account, we will follow the formalism of Tanaka & Ward (2004), generalized by Papaloizou & Larwood (2000) and Cresswell & Nelson (2008) to include high eccentricities, defining a characteristic time-scale,

$$t_{\text{wave}} = \frac{M_p}{M_{\text{emb}}} \frac{M_p}{\Sigma_{\text{gas}} a^2} h^4 \Omega_k^{-1}, \quad (10)$$

$M_p$  is the mass of the planet,  $h = H/r = 0.05$  is the aspect ratio of the disc, and  $M_{\text{emb}}$ ,  $a$ , and  $\Omega_k$  are the mass, the semimajor axis, and the Keplerian frequency of the satellite embryos.

For the time-scales for the migration, eccentricity, and inclination damping, we used the equations from Izidoro et al. (2016), derived from the numerical fits from hydrodynamic simulations found by Cresswell & Nelson (2008), and given by

$$t_{\text{mig}} = \frac{2.0}{2.7 + 1.1\beta} \left( \frac{1.0 + \left(\frac{e}{1.3h}\right)^5}{1.0 - \left(\frac{e}{1.1h}\right)^4} \right) t_{\text{wave}} h^{-2}, \quad (11)$$

$$t_e = \frac{t_{\text{wave}}}{0.780} \left( 1.0 - 0.14 \left(\frac{e}{h}\right)^2 + 0.06 \left(\frac{e}{h}\right)^3 + 0.18 \left(\frac{e}{h}\right) \left(\frac{I}{h}\right)^2 \right), \quad (12)$$

and

$$t_I = \frac{t_{\text{wave}}}{0.544} \left( 1.0 - 0.30 \left(\frac{I}{h}\right)^2 + 0.24 \left(\frac{e}{h}\right)^3 + 0.14 \left(\frac{e}{h}\right)^2 \left(\frac{I}{h}\right) \right) \quad (13)$$

with  $e$  and  $I$  being the embryos eccentricity and inclination while  $\beta$  is the local surface density profile.

From equations (11)–(13), we can write the synthetic accelerations exerted by the disc on to the planet (Cresswell & Nelson 2008) as

$$\mathbf{a}_{\text{mig}} = -\frac{\mathbf{v}}{t_{\text{mig}}}, \quad (14)$$

$$\mathbf{a}_{\text{damp},e} = -2 \frac{(\mathbf{v} \cdot \mathbf{r})}{r^2 t_e} \mathbf{r}, \quad (15)$$

and

$$\mathbf{a}_{\text{damp},I} = -\frac{v_z}{t_I} \mathbf{k}, \quad (16)$$

where  $\mathbf{k}$  is the unit vector in the  $z$ -direction.

The accelerations described in equations (9) and (14)–(16) can easily be translated into the forces presented in the equation (8).

The interaction of the planetary magnetic field with the disc was studied by Takata & Stevenson (1996) and the authors found that the circum-planetary disc is truncated at the co-rotation radius of the planet. Thus, following the prescription of Sasaki et al. (2010) we introduced an inner cavity in the disc at  $\sim 2.25R_J$ , inside this cavity the effects of the gas drag will be neglected.

## 2.5 Hydrodynamic simulations

In this work, we will neglect type II migration because, in our case, the embryos will not become massive enough to open a gap in the disc. The idea that the type II migration could be responsible for the evolution of a satellite system as the Galileans was explored by Miguel & Ida (2016). They argued that in a low viscous disc a gap will be easily opened by the satellites at relatively small masses. Using the results that indicate absence of MRI-active regions in the disc (Fujii et al. 2014, 2017; Turner et al. 2014), Miguel & Ida (2016) choose an  $\alpha$  value between  $10^{-4}$  and  $10^{-6}$ , which we considered excessive small.

To verify the presence of a gap in a low viscous disc, we performed some hydrodynamic simulations to study the evolution of the disc in the presence of a group of satellites with the same mass as the Galileans.

For our hydrodynamic simulations, we used the FARGO 2D package (Masset 2000) with a planet of one Jupiter mass in the centre of the system. We simulate a locally isothermal disc around Jupiter with scale height  $h = 0.05$ ; the disc extends

from  $r_{\text{in}} = 2.25R_J$  to  $r_{\text{out}} = 150R_J$ . The surface density profile adopted was  $\Sigma = \Sigma_0 r^{-3/2}$ , with the initial surface density  $\Sigma_0 = 1.48 \times 10^{-4} M_J / R_J^2$ , such as the disc contains  $2 \times 10^{-2} M_J$ . As the circum-planetary disc must have low viscosity, we used the  $\alpha$ -prescription of Shakura & Sunyaev (1973) with  $\alpha = 5 \times 10^{-4}$ , a value derived for purely hydrodynamic viscosity by the viscous shear instability (Stoll & Kley 2014; Stoll, Kley & Picogna 2017a,b). For the grid resolution, we adopted  $(N_r, N_\phi) = (300, 300)$ .

The four satellites embedded in the disc were initialized with the current mass of the Galileans (see Table 1), in circular orbits and far from their current position, in this way they can migrate through the disc. The accretion of gas by the satellites was neglected because it is believed that these satellites are not composed by gas. The simulation was performed for 150 yr. In Fig. 1, we present snapshots for the evolution of the system for 0, 50, 100, and 150 yr. The structure of the disc is not changed drastically by the presence of the satellites, it is possible to identify some spiral arms near the satellites. These structures are the response of the disc to the presence of bodies, and due to the exchange of angular momentum between the bodies and the disc the satellites migrated inwards.

Our results did not show any sign of gap formation around the satellites. Thus, there is no apparent reason to use the type II regime to describe the migration of the satellites. None the less, we highlight that, due to computational limitation, our simulation only covered the early phases of interaction between the satellites and the disc. A disc with lower viscosity and/or massive satellites might produce different results, but we believe that these conditions are very unrealistic and might lead to an equivocated understanding of the problem.

## 3 RESULTS

In this section, we will present our models and follow the growth and orbital evolution of satellite embryos using different set-ups. In the following, we will explore the impact of some parameters as distribution of the embryos, mass and number of the satellitessimals, the density profile of the gas disc, and the aspect ratio of the disc. A summary of our models is shown in Table 2. The first two models in Table 2 (4-sat-1 and 4-sat-2) describe evolutions of four embryos with the present mass of the Galilean satellites; that is, no mass growth of the embryos by satellitessimals was allowed. The next three models (multi-sat-1, multi-sat-2, and multi-sat-3) start with initially 20 embryos having a small fraction of the mass of the Galilean moons and 2000–2500 satellitessimals that were initially spread throughout the whole disc. In the model multi-sat-uni-1, we simulate the evolution of the system in an uniform gas density nebula ( $\beta = 0$ ) using the same set-up of model multi-sat-1. In the models multi-sat-uni-1-h015, multi-sat-uni-2-h015, and multi-sat-uni-3-h015, we ran the same set-ups of models multi-sat-1, multi-sat-2, and multi-sat-3, respectively, using an uniform gas density with  $\beta = 0$  and a higher aspect ratio,  $h = 0.15$ . In the model (multi-sat-uni-4-h015), we simulate the evolution of satellites in a solid-enhanced disc with uniform gas density, and in the model multi-sat-uni-5-h015, a simulation with uniform gas density and steep distribution of embryos were performed, and for both models,  $h$  was set to  $h = 0.15$ .

### 3.1 Migration of four satellites (model 4-sat-1)

In this model, we will simulate only the migration of a set of massive satellites having the same mass as the Galileans satellites today. The



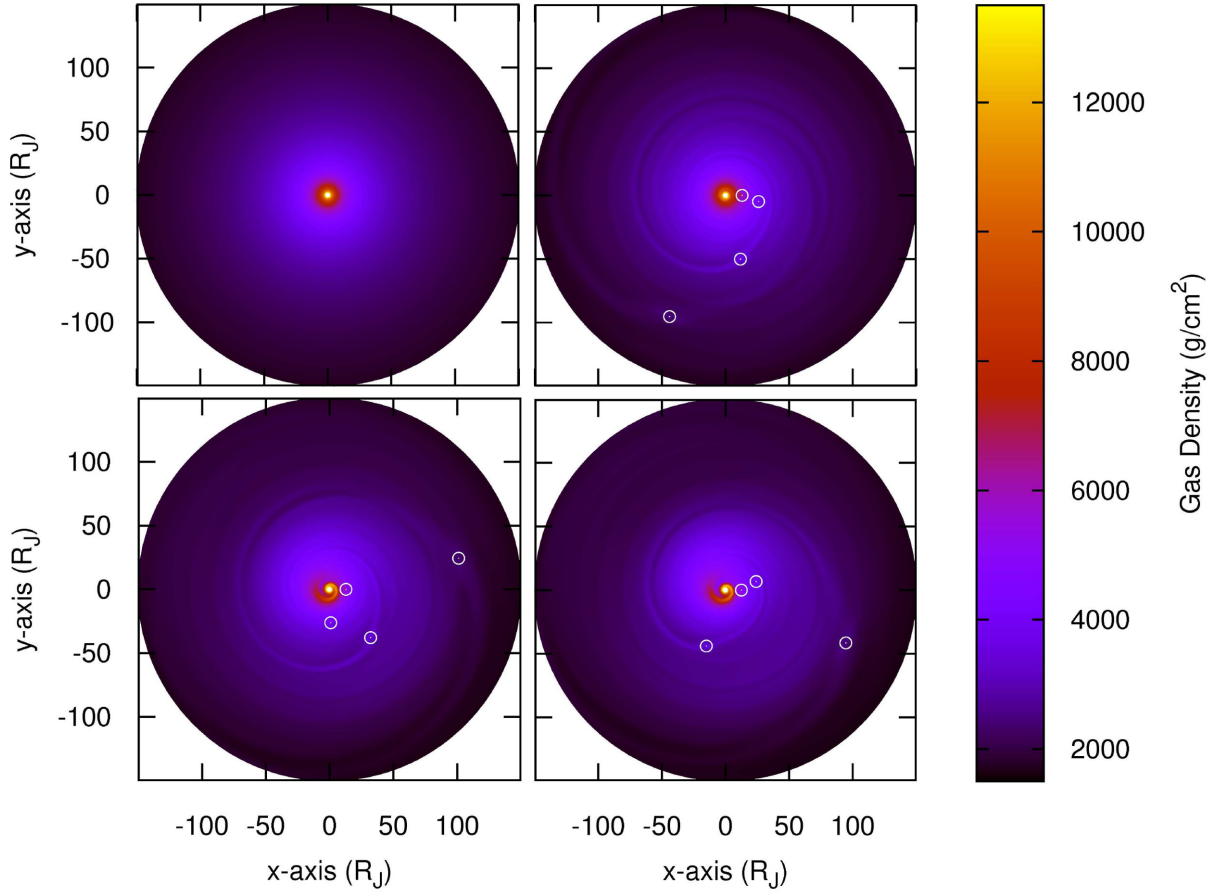


**Figure 1.** Surface density of the disc around Jupiter, after 0, 50, 100, and 150 yr from upper left side to down right side, respectively. The white open circles indicate the position of the satellites.

**Table 2.** Parameters of the simulations. Here, Emb. is the number of embryos; Satel. is the number of satellitesimals;  $M_{\text{emb}}$ ,  $I_{\text{emb}}$ ,  $e_{\text{emb}}$ , and  $a_{\text{emb}}$  are the initial mass, inclination, eccentricity, and semimajor axis of the embryos;  $M_{\text{satel}}$  and  $a_{\text{satel}}$  are the mass and the semimajor axis of the satellitesimals;  $\beta$  is the local surface density profile;  $\frac{M_{\text{gas}}}{M_{\text{solid}}}$  is the gas-to-dust ratio; and  $h$  is the aspect ratio of the disc.

Models	Emb.	Satel.	$M_{\text{emb}}$ $10^{-5} M_J$	$M_{\text{satel}}$ $10^{-5} M_J$	$I_{\text{emb}}$ Deg	$e_{\text{emb}}$	$\beta$	$a_{\text{emb}}$ $R_J$	$a_{\text{satel}}$ $R_J$	$\frac{M_{\text{gas}}}{M_{\text{solid}}}$	$h$
4-sat-1	4	0	2.5–7.8	–	0.0	0.0	1.5	13.4–107.2	–	58	0.05
4-sat-2	4	0	2.5–7.8	–	5.0	0.1	1.5	13.4–107.2	–	58	0.05
multi-sat-1	20	2000	0.04–0.17	0.01	0.0	0.0	1.5	21.0–170.0	21.0–170.0	100	0.05
multi-sat-2	20	2500	0.04–0.17	0.007	0.0	0.0	1.5	21.0–170.0	21.0–170.0	100	0.05
multi-sat-3	20	2000	0.1–0.43	0.007	0.0	0.0	1.5	21.0–150.0	2.25–150.0	100	0.05
multi-sat-uni-1	20	2000	0.04–0.17	0.01	0.0	0.0	0.0	21.0–170.0	21.0–170.0	100	0.05
multi-sat-uni-1-h015	20	2000	0.04–0.17	0.01	0.0	0.0	0.0	21.0–170.0	21.0–170.0	100	0.15
multi-sat-uni-2-h015	20	2500	0.04–0.17	0.007	0.0	0.0	0.0	21.0–170.0	21.0–170.0	100	0.15
multi-sat-uni-3-h015	20	2000	0.1–0.43	0.007	0.0	0.0	0.0	21.0–150.0	2.25–150.0	100	0.15
multi-sat-uni-4-h015	20	2000	0.04–0.17	0.01	0.0	0.0	0.0	21.0–170.0	21.0–170.0	10	0.15
multi-sat-uni-5-h015	20	2000	0.02–0.28	0.01	0.0	0.0	0.0	21.0–170.0	21.0–170.0	100	0.15

surface density of the gaseous disc was described in Section 2. Once we are simulating a phase when the satellites are already formed, it is expected that these bodies performed a previous migration and a portion of the gaseous disc was also dissipated. In this way, we chose the mass of the gaseous disc to be 60 per cent of the total mass proposed by the MMSN model.

Currently, the three inner Galilean satellites are in a 1:2:4 mean motion resonance. This implies a radial separation of a factor of

$\sim 1.6$  from one satellite to another. In our model, the four satellites were initially separated by a factor of 2 from  $13.4R_J$  to  $107.2R_J$ , in circular and coplanar orbits. During the evolution of the satellites, we will check if they can reach the resonant configuration naturally. The results for the semimajor axis and eccentricity evolution are presented in Fig. 2.

The damping in the eccentricity kept the satellites almost circular during the evolution of the system; however, it did not prevent spikes

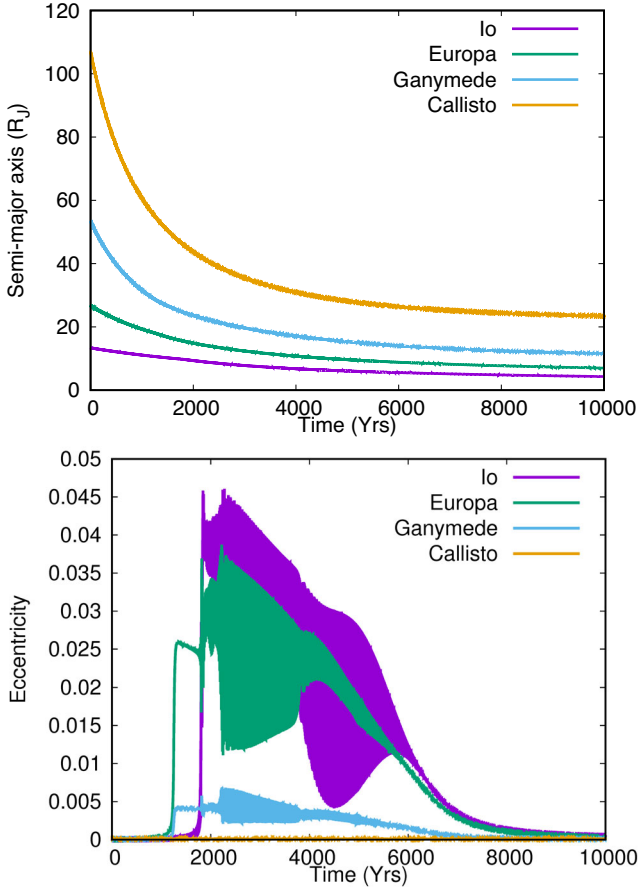


**Figure 2.** Evolution of the semimajor axis and eccentricity of the satellites for model 4-sat-1 over 10 000 yr.

in the eccentricity of Io, Europa and Ganymede, when these bodies reach a resonant configuration.

Due to the interaction with the gaseous nebula the satellites performed an inward migration, the final positions of the satellites from the innermost to the outermost are  $4.31R_J$ ,  $6.85R_J$ ,  $10.9R_J$ , and  $23.3R_J$ , respectively. Once small satellitesimals were not considered, the outer satellites migrated freely through the disc until approach the two innermost ones. At this point, the migration rate of these bodies decreases due to gravitational interaction with the inner satellites and they slowly end in a resonant chain. At the end of the simulation, the three innermost satellites are locked in a 1:2:4 mean motion resonance. As shown by Ogiwara & Ida (2012) at late stages of satellite evolution, the gas surface density would be less denser, such as the damping on eccentricity and semimajor axis will enable the satellites to get lock in multiples 2:1 resonances if the satellites are massive, which is the case here. However, the same authors found that different configurations, with more formed satellites, could yield satellites in different first-order resonant configurations, such as 3:2 and 4:3 for example. We believe that if more than four formed satellites were simulated under the same conditions we used, multiple resonant chains would be found and some of these resonances could be different from 2:1.

Our first scenario is very specific because we assume that the satellites were already formed in circular and coplanar orbits, and the satellitesimal disc was not considered. However, we verify that under such assumptions type I migration is enough to drive the satellites from outer locations to the position of the Jovian satellites.

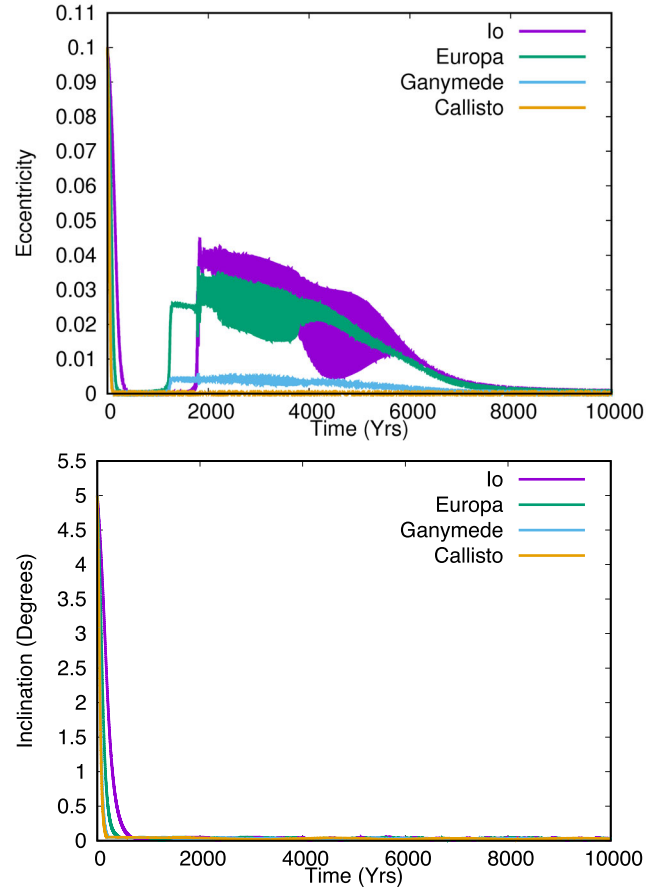


**Figure 3.** Evolution of eccentricity and inclination for the satellites for model 4-sat-2 over 10 000 yr.

### 3.2 Migration of four eccentric and inclined satellites (model 4-sat-2)

To ensure that our results are independent of the assumption of initial circular and coplanar orbits of the satellites, we simulate the same system as before but considering the satellites in orbits with eccentricity of 0.1 and  $5^\circ$  of inclination. The evolution of eccentricity and inclination are shown in Fig. 3.

The values of eccentricity and inclination are damped to almost zero in the first 1000 yr by the damping scheme proposed in the Section 2. After the damping, the satellites remained coplanar until the end of the simulation. The evolution of the eccentricity follows the results from model 4-sat-1. No significant changes were found for the orbital migration of the satellites.

### 3.3 Formation of four satellites (model multi-sat-1)

Now that the migration and damping schemes were tested, we will move to simulations of forming satellites. First of all, the mass of the gaseous disc will be set to  $2 \times 10^{-2}M_J$ , according to the MMSN model. For the solid disc, the mass distribution of individual satellite embryos scales as  $r^{3/4}\Delta^{3/2}$  (Kokubo & Ida 2002; Raymond, Quinn & Lunine 2005; Izidoro, Morbidelli & Raymond 2014), where  $\Delta$  is the number of mutual Hill radii given by

$$\Delta = \frac{a_i + a_j}{2} \left( \frac{M_i + M_j}{3M_p} \right)^{1/3}, \quad (17)$$

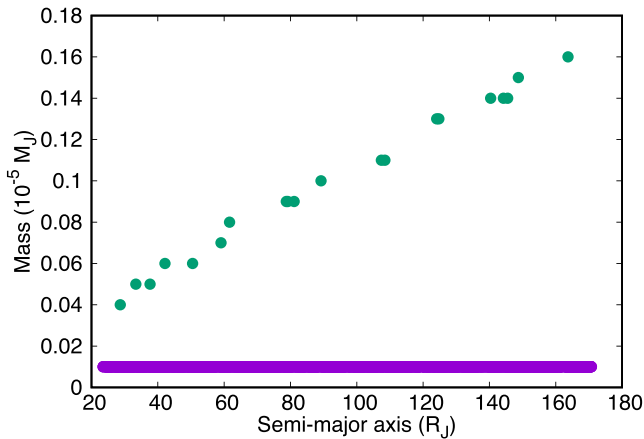


**Figure 4.** Initial mass distribution for model multi-sat-1. Green dots represent the satellite embryos, and purple dots represent the sea of 2000 satellitesimals.

with  $a_i$ ,  $a_j$ ,  $M_i$ , and  $M_j$  being the semimajor axis and mass of two adjacent embryos. The mass of the satellitesimals is constant,  $10^{-7} M_J$ . To reach the solid mass expected by the MMSN model, we simulated 20 satellite embryos and 2000 satellitesimals randomly distributed from  $21R_J$  to  $170R_J$ . In this model, the eccentricity and inclination of all bodies are initially zero, the longitudes were randomly taken between  $0^\circ$  and  $360^\circ$ , and the other orbital elements were set to zero. The initial mass distribution is shown in Fig. 4, where the green dots are the satellite embryos and the purple dots are the satellitesimals. As one can see there is higher initial concentration of massive solids in the outer part of the disc ( $r > 30R_J$ ), even though we did not specify the composition of the satellitesimals, the enhancement in the mass of the solids in the outer disc can be understood as due to ice condensation; however, properly treatment for enhancement due to ice condensation will not be taken into account. Considering that the temperature has a radial dependence as  $T \propto r^{-1}$  and the temperature for ice condensation is about 170 K, the ice line should be located around  $4R_J$ , this topic will be addressed later.

Miguel & Ida (2016) had shown that new generations of satellites are very unlikely to form; these authors adapted their model to add to the system a new embryo seed whenever an embryo collided with the central body; the mass of this embryo seed is 100 times lower than the original embryo; and it is placed at the outer disc. They showed that the solid mass remaining in the disc is not enough to produce a new generation of satellites with mass comparable with the Jovian satellites. For this reason, we neglect the possibility of formation of new generations of satellites if the embryos collide with the planet.

The embryos migrate in the type I regime, while the satellitesimals are dragged by aero-dynamical headwind described in the Section 2. The evolution of the semimajor axis and eccentricity of the satellite embryos are shown in Fig. 5. The migration of the satellite embryos depends on the mass of the embryos and the density of the gaseous; in this way, the embryos initially placed in the inner disc will migrate faster than the ones in the outer disc. Also, the inner embryos tend to accrete more material and become more massive than the outer satellite candidates. Those factors led to the scenario presented in Fig. 5, where the embryos located inside  $120R_J$  migrated faster and collided with the central body, while the outer embryos performed a low migration.

The inner cavity at  $2.25R_J$  should prevent the embryos to fall immediately into the planet; however, with many embryos reaching

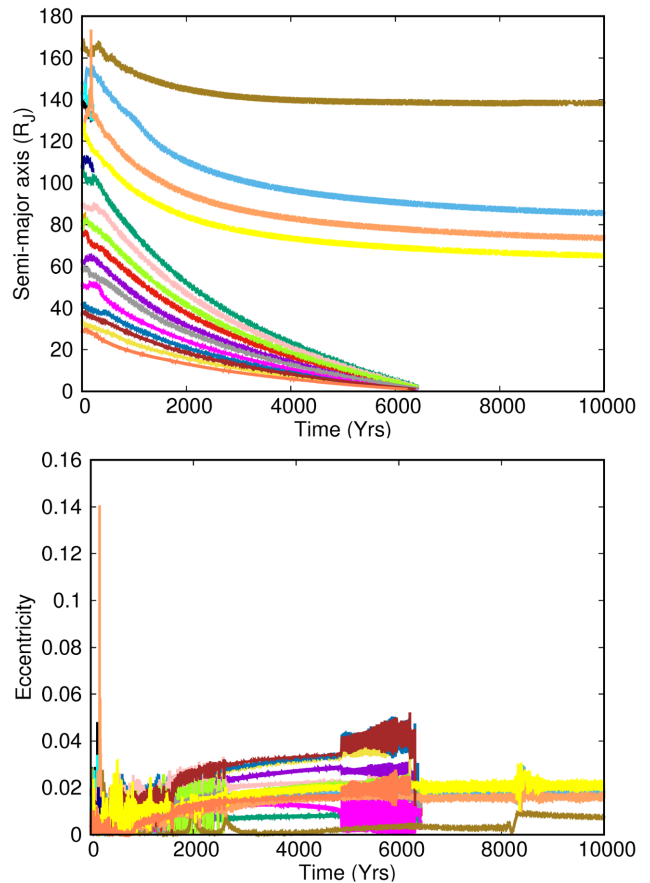


**Figure 5.** Evolution of the semimajor axis and eccentricity of the satellite embryos for model multi-sat-1 over 10 000 yr.

the inner cavity at, roughly, the same time, one embryo will push the other into the planet, causing a series of simultaneous collisions.

The surviving satellites came from the outer disc. Because of the initial density profile of the gaseous disc these bodies were formed in a region poor of gas, which explains the low migration rate presented by them. None the less, the outer bodies were not able to grow to massive satellites once the satellitesimals in the inner solid disc were accreted by the inner embryos or depleted by the gas drag and the interaction with the migrating bodies.

The satellite embryos grow through accretion of solids in their feeding zones, as the embryos migrate their respective feeding zones will move too, providing new material during the embryos evolution. In Fig. 6, we show the mass versus semimajor axis for the formed satellites. The inner embryos became massive faster and migrated towards the planet colliding with the central body. During the migration, these satellites accreted most of the satellitesimals in the inner disc, also the aero-dynamical drag imposed on the satellitesimals contributed for the depletion of part of the solid disc. Because of these factors, the outer embryos that survived are much less massive than the Galilean ones.

Another problem is the mass distribution of the formed satellites. In the Jovian system the two outer satellites are more massive than the inner ones; however, we found it difficult to produce such a distribution in this first model. In our results, the inner satellites are more massive following the trend that inner satellites grow faster and are more massive than the outer ones.

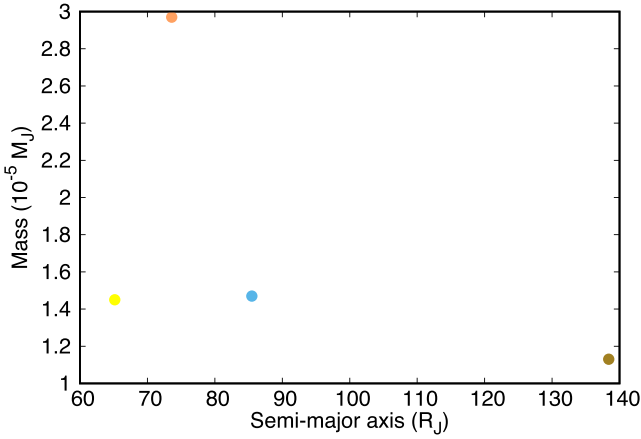


**Figure 6.** Mass versus semimajor axis of satellites formed due accretion of other embryos and satellitesimals for model `multi-sat-1`, after 10 000 yr.

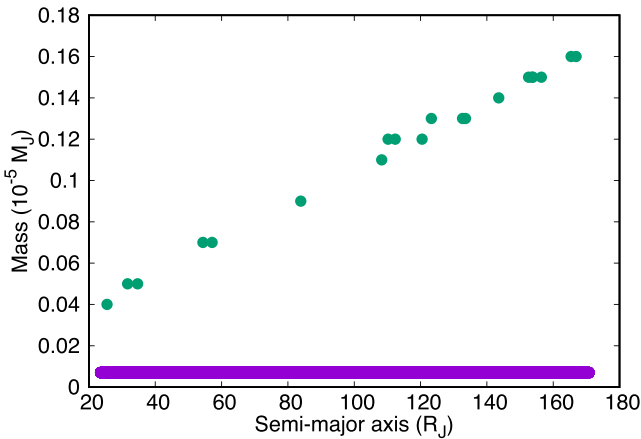


**Figure 7.** Initial mass distribution for model `multi-sat-2`. Green dots represent the satellite embryos and purple dots represent the satellitesimals.

### 3.4 Formation of more than four satellites (model `multi-sat-2`)

The MMSN model assumes the total mass of the solid disc, but how this mass is reached is one of the many uncertainties in the models of satellite formation. In the last model, we opted for a configuration with 2000 satellitesimals and 20 embryos with masses chosen such as the gas-to-dust ratio will be 100. In this model, we will change the number and the mass of the satellitesimals, while the number of embryos will remain the same. The embryos will be once again randomly distributed, while the other parameters of the disc will be the same as in model `multi-sat-1`. We simulate 2500 satellitesimals with  $7 \times 10^{-8} M_J$  each (see Fig. 7 for the initial distribution of the bodies). Our goal is to show how sensitive to the initial conditions this system can be.

At the end of the simulation, five satellites were formed in orbits close to each other (Fig. 8). A final configuration with more than four satellites is not so uncommon and was previously reported by Sasaki et al. (2010), for example. As we know from our previous model, the number of formed satellites is strongly influenced by the initial distribution of the embryos, as only embryos initially located beyond  $120 R_J$  became satellites. In this model, the random distribution of the embryos placed more bodies beyond  $120 R_J$  than in the model `multi-sat-1`, which might explain the formation

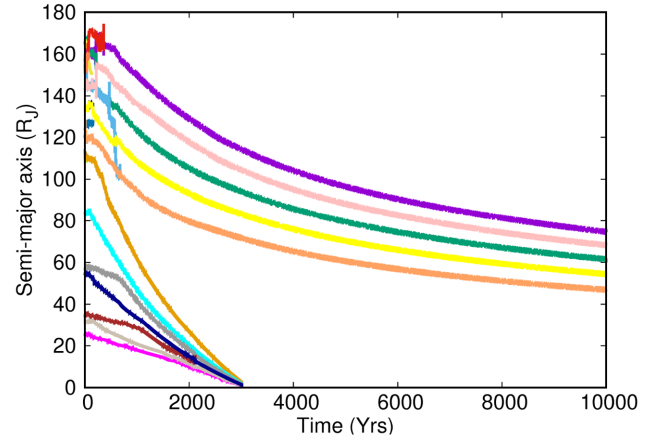


**Figure 8.** Evolution of the semimajor axis of the satellites embryos for model `multi-sat-2`, after 10 000 yr.

of five satellites instead of four. We also performed simulations with the same distribution of embryos as in model `multi-sat-1`, changing the mass and number of satellitesimals (not showed here) and we found only four surviving satellites with configuration more compact than in the model `multi-sat-1`.

In Fig. 8, the orbital migration of the satellites embryos is shown. The general evolution is somehow similar to the one found in the model `multi-sat-1`. The embryos located at the inner regions of the disc grow faster through accretion of satellitesimals and they rapidly migrated towards the planet, after reaching the inner edge of the disc they collide with the central body. On the other hand, the migration of bodies from the outer disc is slower, because this is a region of low density and, at this point, the bodies are generally less massive than the ones from the inner disc. Comparing with the system formed in the model `multi-sat-1` the system in this model is more compact and is located inside  $80 R_J$ , this configuration is a product of the initial distribution of the embryos and the interaction between the embryos in the outer disc. The initial number of satellitesimals is important only in the first phases of embryos growth, especially for the inner ones, these embryos grew faster than in the previous model and fell into the planet. For the outer embryos, the effects of having more satellitesimals in the systems was not relevant. The final mass distribution of the satellites is similar to the distribution presented in the model `multi-sat-1`, with the second innermost satellite being the most massive one and the outermost satellites being less massive (Fig. 9). The increase in the number of satellitesimals was not enough to change this scenario, once the location of these new bodies was randomly selected. This tendency raises questions about how the Galileans reach their final masses, especially Ganymede and Callisto.

### 3.5 Formation of several satellites in resonance (model `multi-sat-3`)

So far we have shown results when systems with four or five satellites were formed; however, the number of final satellites depends of the initial distribution of the embryos. We found that distributions with more embryos in the outer disc tend to produce systems with more satellites. The bodies formed in the previous models were not as massive as the Galileans and were located far from the regions of the regular satellites of Jupiter. In this model, we will change the size of the disc and the initial mass of the satellite embryos.



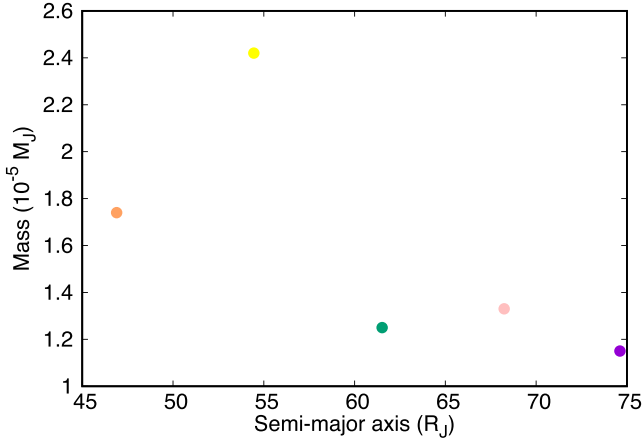


**Figure 9.** Mass versus semimajor axis of satellites formed due accretion of other embryos and satellitesimals for model multi-sat-2, after 10000 yr.

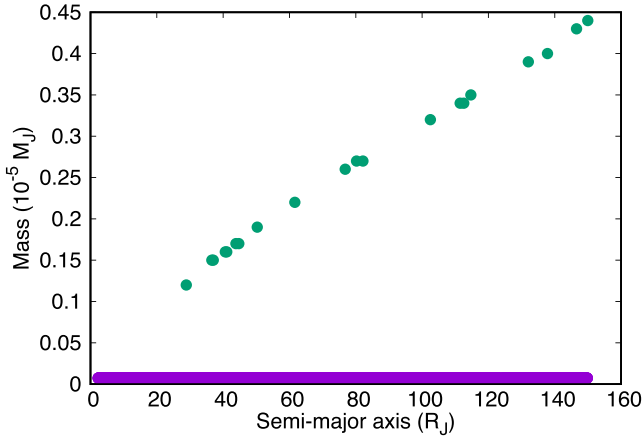


**Figure 10.** Initial mass distribution for model multi-sat-3. Green dots represent the satellite embryos and purple dots represent the satellitesimals.

We will simulate 2000 satellitesimals with mass  $7 \times 10^{-8} M_J$ , randomly spread from  $2.25 R_J$  to  $150 R_J$  and 20 satellite embryos with approximately three times the initial mass used in the previous two models, these bodies are distributed from  $21 R_J$  to  $150 R_J$ . This new set-up is an attempt to solve the problem of formation of satellites with low mass at large distances. If the outer satellites become massive they could migrate to the inner regions of the disc. The initial solid mass distribution is presented in Fig. 10, where the green points are the satellite embryos and the purple points are the satellitesimals.

The orbital evolution of the satellite embryos is shown in Fig. 11. The migration of the embryos follows the trend of the previous model, the embryos inside  $120 R_J$  migrate faster and reach the inner edge of the disc, while the embryos located beyond  $120 R_J$  performed a slow migration. Different from the previous simulations the satellites did not collide with the central body, they piled up close to the inner cavity in a resonant configuration. In fact, when the inner cavity is placed at the co-rotation radius of the planet the tendency is that a satellite halts its migration and does not fall into the planet. However, the approach of multiple satellites almost at the same time might push the inner satellites towards the planet causing the loss of these bodies, as in the previous models. In this simulation, the migration speed of the satellites was lower compared to the

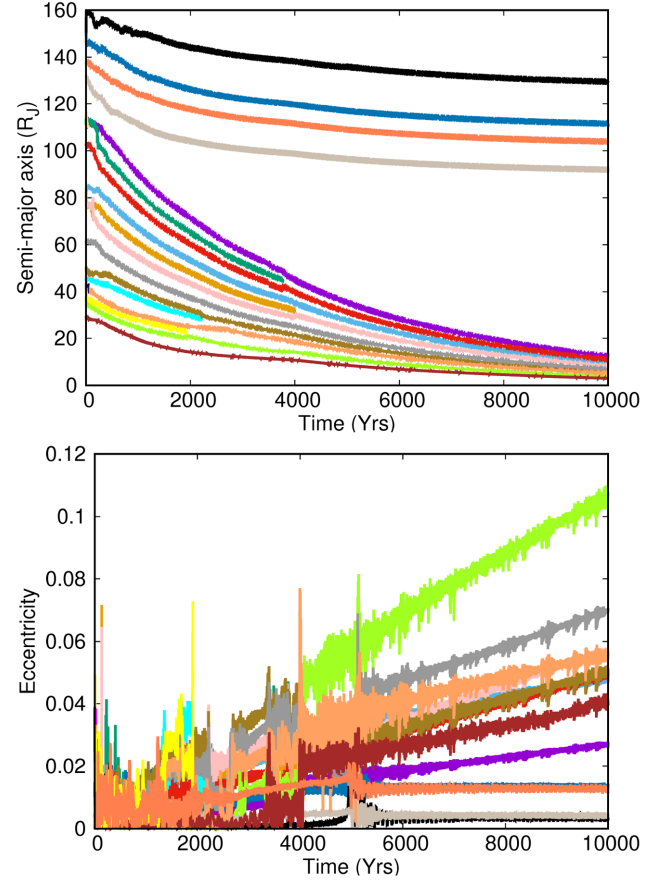


**Figure 11.** Evolution of the semimajor axis and eccentricity for the satellites for model multi-sat-3 after 10 000 yr.

models multi-sat-1 and multi-sat-2, because most of the satellites inside  $120 R_J$  entered in a resonant configuration instead of falling into the planet. After the resonant scenario be achieved the migration continued until the inner bodies reach the cavity.

Recent studies demonstrate that dissipation of the gaseous disc generates instabilities between close bodies in resonance, leading to the break-up of possible resonant chains (Izidoro et al. 2017). In our model, the gaseous disc dissipates exponentially (equation 5). Thus, the instabilities are expected and the resonant chains between the close satellites might not hold. In our results, the eccentricity of the inner satellites increases because of the compact configuration of these bodies (the bottom panel of Fig. 11), the instabilities generated by the dissipation of the gaseous disc also affects the satellites; however, the resonant configuration is not broken until the end of our simulation. In this compact configuration, the break-up of the resonant chains will produce several collisions between the satellites. A similar behaviour was observed for super-Earth systems, where multiple planets piled up in resonant chains near the star; however, in this case, the instabilities due to the gas dissipation breaks these chains and the planets start to collide with each other or fall into the star (Izidoro et al. 2017).

The system of four satellites formed in the outer disc also presents a resonant configuration; however, it is not expected that this configuration will be broken by instabilities due to gas dissipation. The gas density in the outer disc is already low and the dissipation of this disc will produce only weak instabilities that should not be strong enough to break the resonant chains between the satellites.

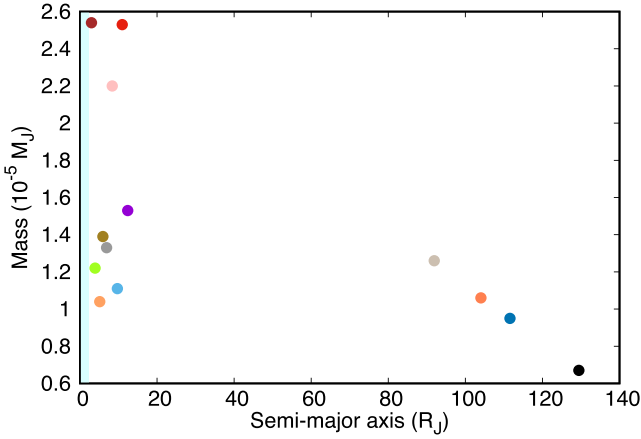


**Figure 12.** Mass versus semimajor axis of satellites formed due accretion of other embryos and satellitessimals for model *multi-sat-3*, after 10 000 yr. The cyan region represents the inner cavity of the disc.

This physical argumentation is supported by simulations involving super-Earth systems in the literature.

In Fig. 12, we show the final radial mass distribution of the satellites. It is possible to see the inner satellites piled up close to the inner cavity. As in the previous models, most of the inner satellites are more massive than the outer ones.

The formation of numerous satellites shows the dependency on the initial conditions, in particular the radial distribution and the masses of the embryos. However, the biggest question that remains concerns the final masses of the satellites, so far all the formed systems have masses lower than the mass of the Galileans. Possible solutions include considering a solid and/or gas disc more massive than the predicted by the MMSN or change the density profile avoiding the fast migration of the inner embryos and decreasing the depletion of the satellitessimal disc.

The final configuration of the system and the resonant chains formed during the evolution of the satellites resembles the evolution of super-Earth planets around solar mass stars (Izidoro et al. 2017). From our findings, it is possible to argue that satellite systems such as the Galileans might have a formation pathway similar to a planetary system with super-Earths around a solar mass star on a different scale.

### 3.6 Growth and migration of satellites in a uniform gas disc (models *multi-sat-uni-1*)

There are many uncertainties concerning the density profile of the gaseous disc; for simplicity, we adopted a power-law profile with index  $\beta = 3/2$ . This profile was chosen in order to have more material in the inner disc, as it might be expected due to the inflow of material from the proto-planetary disc to the planet. However, the profile implies a fast migration of the inner embryos and slow migration of the outer ones, also the satellitessimals in the inner disc are depleted faster due to the high density in this region. For comparison, we present in this section a model in which we use an initial uniform gaseous disc with  $\beta = 0$ . To ensure a fair comparison, the initial conditions of the embryos and the solids configuration will be the same as in model *multi-sat-1*.

With an initial uniform distribution of the gas it is expected that the migration rates of the satellite embryos to become more similar, decreasing the possibility of formation of satellite in the outer parts of the disc. Also, in the case of formation of resonant chains, the

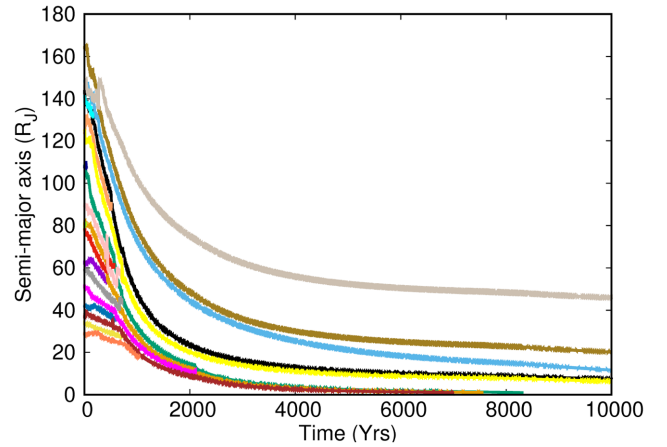


**Figure 13.** Evolution of the semimajor axis of the satellites embryos for the model *multi-sat-uni-1* after 10 000 yr.

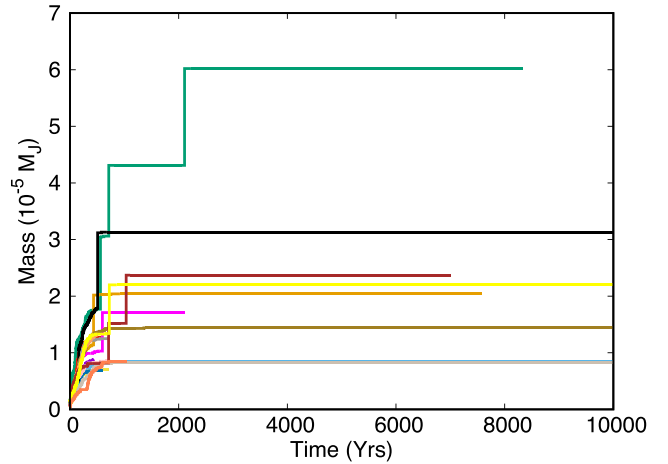


**Figure 14.** Evolution of the mass of the satellitessimals for the model *multi-sat-uni-1* after 10 000 yr.

dissipation of the gaseous nebula might have a similar effect in the inner and outer disc.

The orbital migration of the satellite embryos for our model is shown in Fig. 13. Different from the models where the gas distribution has a radial dependence, now the embryos from the outer disc migrate faster changing the general migration of the inner embryos. We can notice that due to the migration of the outer embryos several collision took place well before 1000 yr. At the end of the simulations, we have five surviving satellites, with the outermost one being inside  $50R_J$ , while the other four are distribute from  $6R_J$  to  $27R_J$ . These final locations for the satellites reproduce the location of the Galilean satellites better than our previous models.

The final mass of the formed satellites remains an issue. In Fig. 14, we show the mass evolution of the embryos. Most of the satellitessimals are accreted in the first 500 yr, the satellitessimals that are not accreted in this stage are scattered by the migrating embryos. The collision between embryos also contribute for the growth of the final satellites. After approximately 2000 yr, there is no much change in the masses of the remaining satellites for our model. The satellites in this models reached masses from  $0.83 \times 10^{-5}M_J$  to  $3.1 \times 10^{-5}M_J$ . However, we can see in Fig. 14 that massive satellites, around  $6 \times 10^{-5}M_J$ , were formed during the evolution of the

system; unfortunately, this satellite was lost due to collision with the central planet.

Simulations with  $\beta = 1/2$  and  $\beta = 1.0$  were also performed. We decided not shown these results because in both cases the surviving satellites are located in the region between the satellites formed with  $\beta = 0$  and  $\beta = 3/2$  and are not as massive as the satellites formed with uniform distribution. These behaviours indicate that, under our assumptions, flatter gas discs are more favourable for the formation of satellites in the inner disc.

### 3.7 Models with higher aspect ratio (models multi-sat-uni-1-h015, multi-sat-uni-2-h015, and multi-sat-uni-3-h015)

In the last section, we approached the problem of fast migration of the innermost satellites changing the initial distribution of the gas density, the results shown an improvement in the migration but not in the masses of the final satellites. In this section, we will address the questions about the temperature in the disc.

In our models, we are not interested in developing a very sophisticated temperature profile; however from equation (7), we estimated that the ice line (when the temperature is  $\leq 170$  K) is around  $4R_J$ , which is very close to the planet. The initial temperature of the disc is given by

$$T_0 = \frac{h^2 G M_p \mu}{\mathcal{R}}, \quad (18)$$

where  $G$  is the gravitational constant,  $\mu$  is the average molecular weight, and  $\mathcal{R}$  is the gas constant. Thus, the initial temperature can be changed modifying the value of the aspect ratio  $h$ , consequently is possible to initially place the ice line in a more reliable location. Following the work by Lunine & Stevenson (1982) and Miguel & Ida (2016), for example, the ice line is predict to be located around  $30R_J$ ; to match this value, we set the aspect ratio as  $h = 0.15$  (an intermediate value could be chosen for the aspect ratio, let us say 0.1; however, it will not move the ice line to  $30R_J$ ). As a consequence for increase the value of  $h$ , the migration rate of the satellites should decrease because the disc becomes thicker, in this way, and based in the results from last section, we opt to use an uniform gas density profile. Our simulations will have the same initial conditions as the models multi-sat-1, multi-sat-2, and multi-sat-3, only changing the gas density profile and the aspect ratio, as specified before. To avoid complications, we will name our new models as follows, the model multi-sat-uni- $i$ -h015 will have the same initial configuration as model multi-sat- $i$  with an initial uniform distribution for the gaseous disc and a  $h = 0.15$ , where  $i = 1, 2, 3$ .

Fig. 15 shows the evolution of the semimajor axis of the embryos for the models multi-sat-uni-1-h015, multi-sat-uni-2-h015, and multi-sat-uni-3-h015. As expected, the migration rate of the embryos decreased compared with the model multi-sat-uni-1; for all three models, the inner satellites are distributed from around  $20R_J$  to  $60R_J$ , while the outer ones were formed beyond  $80R_J$ . Similarly to model multi-sat-uni-1, the evolution of the embryos here was determined by multiple collisions between each other, specially in model multi-sat-uni-1-h015 where only four satellites were formed with no first-order resonance holding them together. For the other two models (multi-sat-uni-2-h015 and multi-sat-uni-3-h015), we have four and five satellites forming in the inner group and two satellites forming in the outer group, also a small number of first-order reso-

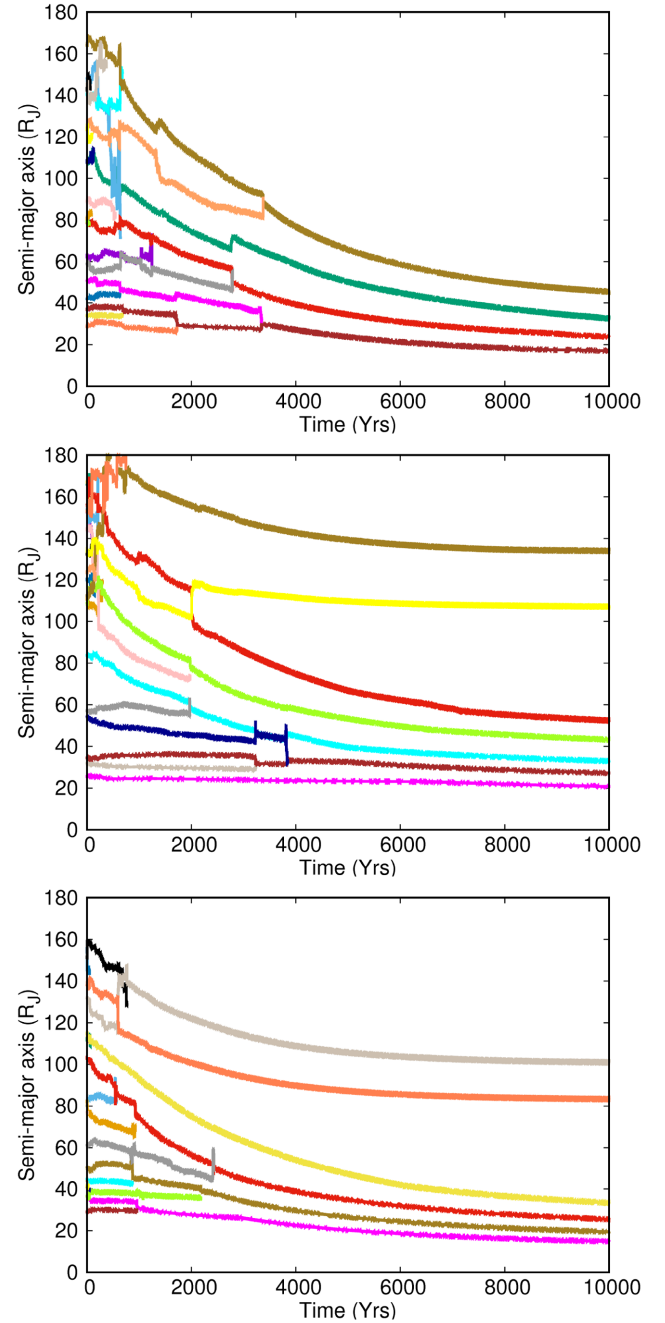


**Figure 15.** Evolution of the semimajor axis of the satellites embryos for the models multi-sat-uni-1-h015, multi-sat-uni-2-h015, and multi-sat-uni-3-h015 after 10 000 yr, respectively, from top to the bottom.

nance chains were found for the satellites located in the inner group in both models.

The final radial distribution of mass for our models is shown in Fig. 16. We highlight the enhancement in the masses of the formed satellites in the models multi-sat-uni-1-h015 and multi-sat-uni-3-h015; the most massive satellite is almost as massive as Ganymede, while in the model multi-sat-uni-2-h015 the most massive satellite has a mass comparable to Io. These models are the only models presented so far that produced satellite with masses comparable with the Galileans.

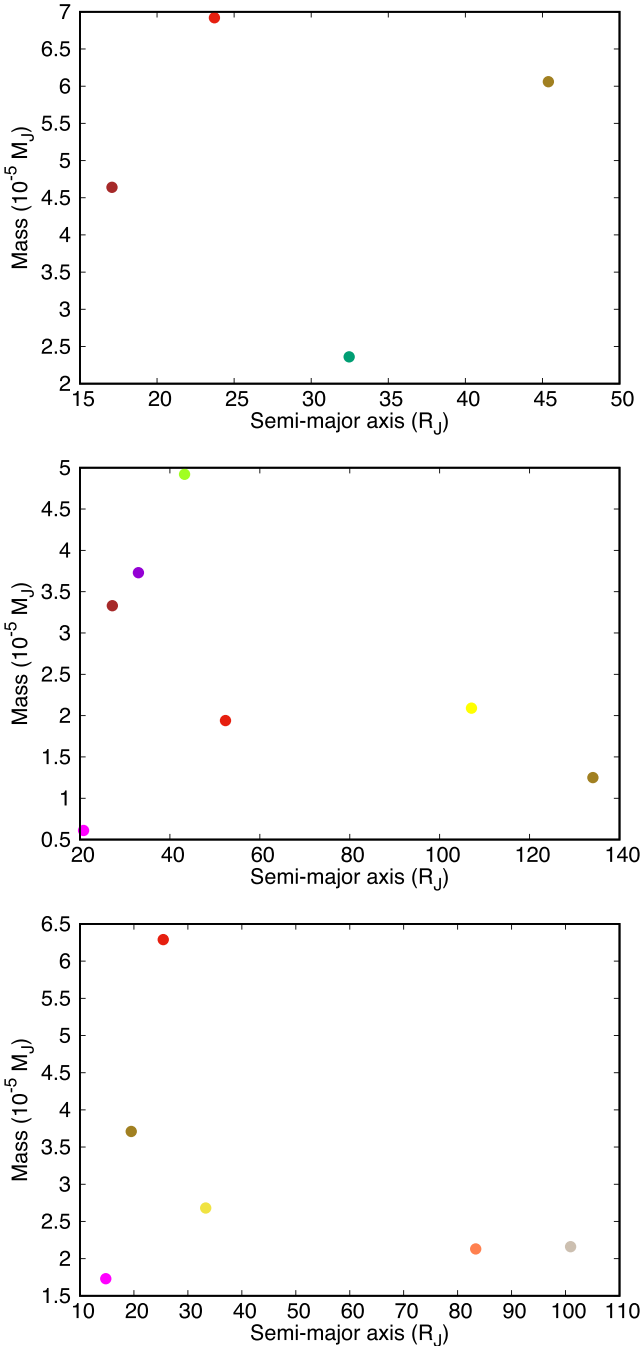


**Figure 16.** Mass versus semimajor axis of satellites formed due to accretion of other embryos and satellitessimals for models multi-sat-uni-1, multi-sat-uni-2, and multi-sat-uni-3 after 10000 yr, respectively, from top to bottom.

The model multi-sat-uni-1-015 was capable to reproduce the masses of the Galileans satellites very accurately, where Io was reproduced by the first satellite, Ganymede was reproduced by the second one, Europa was reproduced by the third one, and Callisto was reproduced by the fourth satellite (ordering our satellites from the innermost to the outermost). The only issue are the switched position between the Ganymede analogous and the Europa analogous, and the fact that our group of satellite is not in the exactly location of the Galilean satellites.

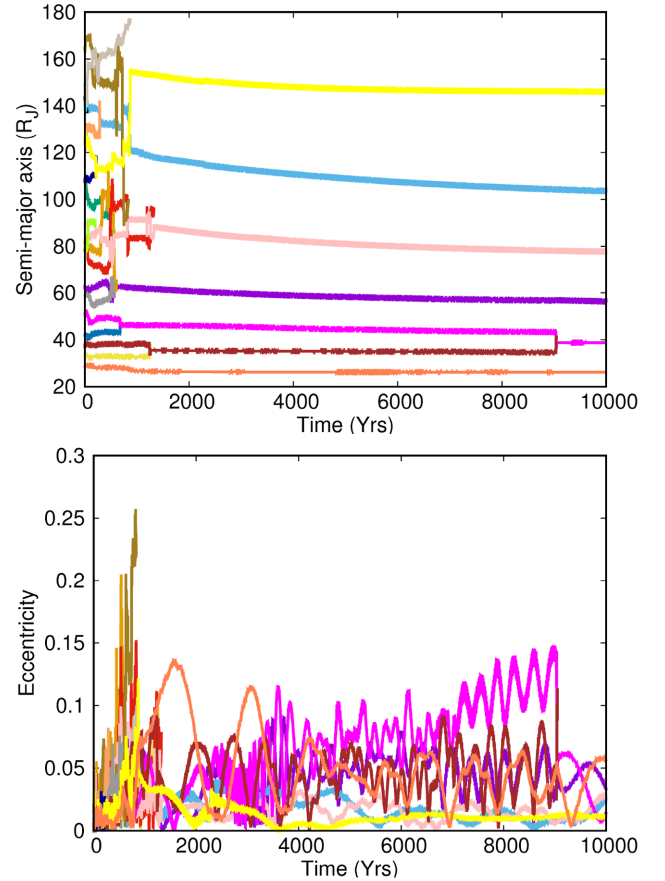


**Figure 17.** Evolution of the semimajor axis and eccentricity for the satellites for model multi-sat-uni-4 after 10000 yr.

Even though the position of the formed satellites was not well reproduced, the increase in the aspect ratio of the disc was crucial for the improvement in the mass of the satellites; here, we could reproduce the masses of the Galileans and see that our approach to the problem can generate massive satellites once the position of the ice line is moved to around  $30R_J$ . In this way, we will use the same aspect ratio and gas density distribution for the upcoming models.

### 3.8 Model with a solid-enhanced composition (model multi-sat-uni-4-h015)

In our previous models, we changed the number and mass of embryos and satellitessimals always keeping the gas-to-dust ratio to be 100. However, different ratios can be tested under the MMSN assumptions. Here, we decide to test a model with a higher concentration of solids; in this way, we will build a disc with gas-to-dust ratio of 10.

We will use the model multi-sat-uni-1-h015 as a reference for the initial conditions. In order to enhance the concentration of solids, we preserve the original amount of solids and remove a certain amount of gas from the disc until the gas-to-dust ratio becomes 10. In this way, we are still considering a minimum mass disc model for solids. Differently to Mosqueira & Estrada (2003b) and Estrada et al. (2009), we choose to decrease the gas density in all parts of the disc equally, not giving preference for a specific region.

In Fig. 17, we show the evolution of semimajor axis and eccentricity for the model multi-sat-uni-4-h015. The reduction



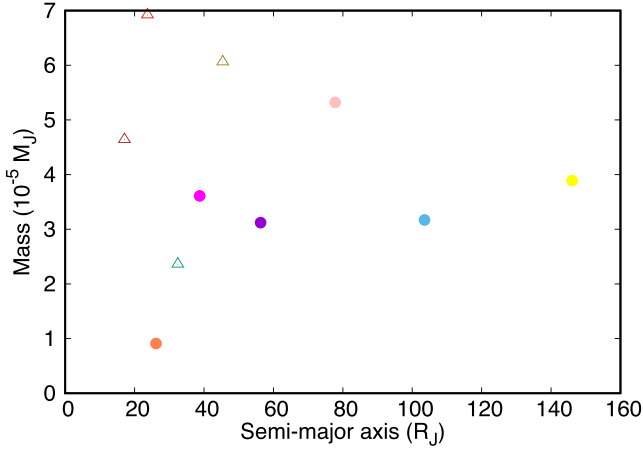


**Figure 18.** Comparison of the final mass distribution of satellites formed due accretion of other embryos and satellitesimals for the models *multi-sat-uni-4-h015* (filled circles) and *multi-sat-uni-1-h015* (asterisk marks) after 10 000 yr.

of the gas in the nebula slow the migration rate of the embryos, such that the number of satellites formed is higher compared with the model *multi-sat-uni-1-h015*, also the formed satellites are located farther away in the disc. Only one 3:2 resonance chain was found locking the fourth and fifth outermost satellite.

Fig. 18 shows the comparison between the final mass distribution of the satellites for the models *multi-sat-uni-4-h015* and *multi-sat-uni-1-h015*. We can see that the values of masses for the model *multi-sat-uni-4-h015* are slightly smaller than in the model *multi-sat-uni-1-h015*, probably because of the formation of more satellites. The masses of the satellites in this model are more compatible with the masses of model *multi-sat-uni-2-h015*.

### 3.9 Model with a uniform gas disc and an steep distribution for the embryos (model *multi-sat-uni-5-h015*)

So far we treated the embryos distribution such as it scales as  $r^{3/4} \Delta^{3/2}$ ; however, this distribution depends on the slope of the surface density distribution. In this way, for uniform distributions as discussed in the models *multi-sat-uni-1* and *multi-sat-uni-i-h015*, the distribution of the embryos should scale differently. To cover this, in this section we will run a simulation with the same set-up as model *multi-sat-uni-1-h015* with the embryos distribution proportional to  $r^3$  (Kokubo & Ida 2002; Raymond et al. 2005; Izidoro et al. 2014). The initial distribution of the embryos (and the satellitesimals) is shown in Fig. 19, as the distribution is steeper, the difference in mass between the more massive and the less massive embryo is greater than found in the previous models.

The migration of the embryos followed the pattern found for the models with uniform surface density, six satellites survived inside  $13.5R_J$  and  $87R_J$  (Fig. 20). Only two 3:2 resonant chains were found, which is the most common commensurability in our simulations. As we pointed before, the initial distribution of the embryos changes the final number of satellites; however, their final location is an outcome of the gas density profile and the scale height.

Fig. 21 shows the final distribution of mass of the surviving satellites. Following the trend of the models with uniform surface density, the satellites are more massive than the ones from simulation with  $\beta = 3/2$  and  $h = 0.05$ . Comparing exclusively with the

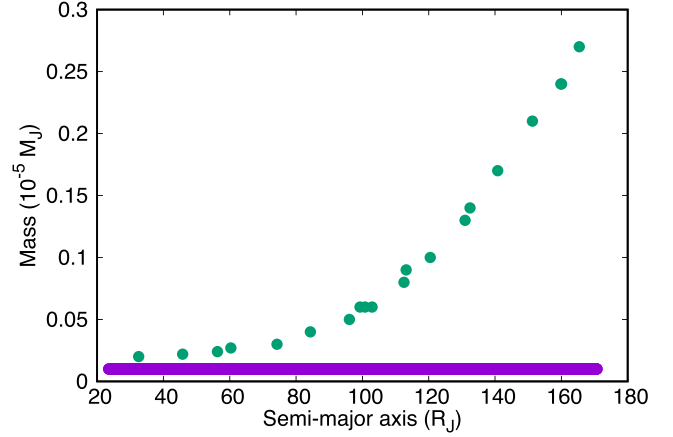


**Figure 19.** Initial mass distribution for model *multi-sat-uni-5*. Green dots represent the satellite embryos and purple dots represent the satellitesimals.

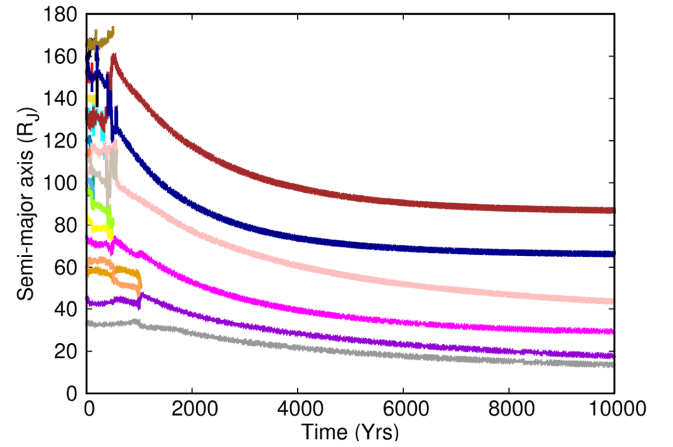


**Figure 20.** Evolution of the semimajor axis for model *multi-sat-uni-5-h015* after 10 000 yr.

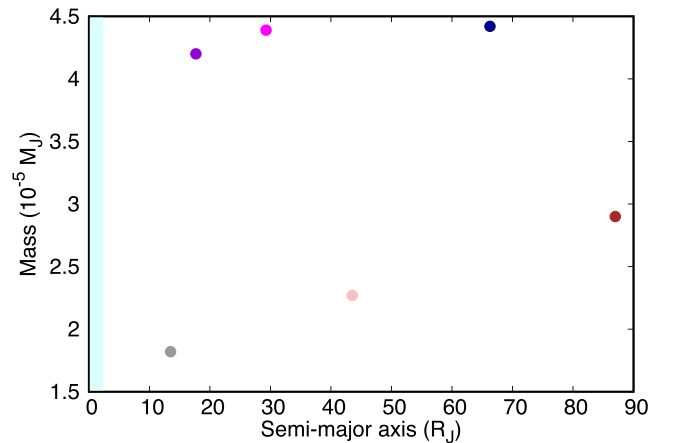


**Figure 21.** Mass versus semimajor axis of satellites formed due accretion of other embryos and satellitesimals for model *multi-sat-uni-5-h015* after 10 000 yr. The cyan region represents the inner cavity of the disc.

**Table 3.** Summary of our results. Here,  $a$ ,  $M$ , and  $e$  are the range of values for the semimajor axis, mass, and eccentricity of the satellites, and in the last column, the number of satellites in first-order resonances (2:1, 3:2, 4:3, 5:4, 6:5, and 7:6).

Models	Satellites	$a$ $R_J$	$M$ $10^{-5} M_J$	$e$	First-order MMR
4-sat-1	4	4.31–23.3	2.5–7.8	0.0001–0.0005	3
4-sat-2	4	4.31–23.3	2.5–7.8	0.0001–0.0005	3
multi-sat-1	4	65.2–138.4	1.1–3.0	0.0075–0.02	3
multi-sat-2	5	46.9–74.6	1.1–2.4	0.011–0.029	4
multi-sat-3	13	2.99–29.6	0.67–2.5	0.004–0.11	12
multi-sat-uni-1	5	6.35–46.0	0.83–3.1	0.0002–0.026	2
multi-sat-uni-1-h015	4	17.0–45.4	2.36–6.97	0.01–0.095	0
multi-sat-uni-2-h015	7	20.8–134.0	0.61–4.92	0.022–0.15	4
multi-sat-uni-3-h015	6	14.8–101.0	1.76–6.29	0.115–0.036	3
multi-sat-uni-4-h015	6	26.2–146.1	0.91–5.3	0.011–0.056	1
multi-sat-uni-5-h015	6	13.5–87.0	1.82–4.42	0.012–0.12	2

model `multi-sat-uni-1-h015`, the final masses of the satellites are smaller, even though some of these satellites started with a higher initial mass and the process of capture of satellitesimals and small embryos was easier, probably the formation of more than four satellites was the reason they do not became more massive. None the less, it is important to notice that even the most massive satellite produced in this model is only comparable to Io, highlighting the difficulties to create satellites as massive as Ganymede and Callisto.

### 3.10 Close-in super-Earths systems versus multiple satellites systems

The comparison between the formation of the Galilean system with the formation of planets in our Solar system is not something new; however, the better match may be found amongst the extrasolar planets. The close-in super-Earths are planets with masses of  $\sim 10^{-5}$ – $10^{-4} M_\odot$  orbiting close to the host star, with orbital periods shorter than 100 d (Mayor et al. 2011; Howard et al. 2012; Petigura, Howard & Marcy 2013). It is believed that the close-in super-Earths were formed in a circum-stellar disc and accrete only solid materials analogous to the Galilean satellites; in addition, the super-Earths have the same mass ratio as the Jovian satellites (Sasaki et al. 2010).

Recently, the studies about the formation of close-in super-Earths received a boost with the confirmation of seven Earth-size planets with very short orbital periods in the TRAPPIST-1 system (Gillon et al. 2016, 2017), some of them in resonance (Luger et al. 2017). Studies, such as Ormel, Liu & Schoonenberg (2017) and Izidoro et al. (2017), were performed looking for a better understanding about formation and evolution of super-Earths systems, in general, using resonant chains as a constraint for the problem.

The model proposed by Izidoro et al. (2017) showed the possibility of formation of multiple planets close to the star in resonance and how this resonance could be broken due to instabilities. Comparing their results with ours, in particular model `multi-sat-3`, we can see that the formation of resonant chains in systems with multiple super-Earths is also found in systems with multiple satellites close to each other. Izidoro et al. (2017) pointed that the dissipation of the gaseous nebula induces instabilities in the planetary orbits that breaks the resonant chains leading to several collisions between the planets. This behaviour was not found for satellites, once the evolution of the system was finished with the satellites locked in resonances. The final resonant configurations of the satellites might be a consequence of the small mass of these bodies. Also, the high eccentricity presented by the super-Earths in resonance was similar for the satellites.

Despite the general similarities in the models and results, we stress that for super-Earths systems the turbulence in the disc plays an important role, while for satellites the disc is usually considered to be laminar.

In this section, we are comparing only the dynamical evolution of satellites and super-Earths, we do not claim that every feature of the formation process is the same. It is known that the composition of super-Earths and satellites can be very different, which means that their formation discs were different; however, the inward migration, the formation close to the central body, and the resonant chains indicate that they experienced similar evolutions. In this way, the results for satellites in a circum-planetary disc can be scaled for super-Earths in a proto-planetary disc.

Table 3 shows a quick summary of our result with the number of satellites formed, range of final semimajor axis, mass and eccentricity of the satellites, and the number of satellites in first-order resonances.

## 4 CONCLUSIONS

We have investigated the growth and orbital evolution of satellite embryos in a circum-planetary disc around a giant planet with the characteristics of Jupiter. For this purpose, we used dedicated  $N$ -body simulations including the effects of type I migration, eccentricity, and inclination damping for the embryos and gas drag for the satellitesimals. We simulated a massive, low viscosity disc consistent with the studies regarding MRI regions in Jupiter's circum-planetary disc; we also did not consider any infall of material on to the disc. We performed multiple simulations changing the distribution and the masses of the embryos as well as the number and masses of the satellitesimals in the disc.

Previous work on the formation of the Galilean satellites used the type II migration regime (Miguel & Ida 2016). To verify this possibility, we simulated the migration of four massive satellites in a circum-planetary disc using two-dimensional hydrodynamic simulations over 150 yr. Our results showed no signs of a gap being opened by the satellites, thus the use of type II migration in this problem is hard to justify. In our hydrodynamic simulations, we considered  $\alpha = 5 \times 10^{-4}$  for the viscosity prescription, in agreement with recent values for purely hydrodynamic turbulence in discs (Stoll & Kley 2014; Stoll et al. 2017a,b).

The  $N$ -body simulation with fully formed satellites (having the mass of the Galileans) showed that our integration scheme is capable of reproducing the migration of massive satellites from the outer parts of the disc to a configuration that resembles the current

architecture of the Galilean satellites. In addition, we showed that, for massive satellites, initially eccentric and inclined orbits do not affect the final results due to the damping in the disc. The satellite embryos formed in the outer disc would be enriched with icy materials, as observed, which is in agreement with our simulations that initially have more massive embryos present in the outer parts of the disc.

From the simulations with satellite embryos and satellitessimals we found that the final number of formed satellites depends on the initial distribution of embryos in the disc. Embryos initially located at the outer disc are more likely to survive and become satellites, while the inner embryos tend to migrate faster and collide with the central body due to the high gas density in this region. Also, we showed that most of the satellitessimals in the disc are accreted by the inner embryos or depleted during the migration phase of the embryos; in this way, the growth of massive satellites from the outer disc is more difficult. An inflow of mass as proposed in the gas-starved disc (Canup & Ward 2002, 2006, 2009) might favour the formation of satellites from the outer disc; also, the inflow of material could help the outer satellites to become more massive than the ones we found. The gas-starved disc scenario and the possibility of inflow of mass were not addressed in this work, since we were interested in the study of the evolution of satellites in a static, massive disc. However, even though no inflow of material is a general assumption for the MMSN model, hydrodynamic simulations have shown that this is not completely true and inflow of material from the ambient protoplanetary disc might be possible. In this way, our models could be improved in the future by adding this effect.

When we simulated more massive embryos, we found a configuration with multiple small satellites close to the planet. These satellites are locked in resonant chains that remain stable after the gas disc dissipates, while the eccentricity of the satellites increased due to their proximity. Similar behaviour has been seen in simulations for extrasolar close-in super-Earths systems (Izidoro et al. 2017), with the difference that after the gas dissipation the planets start to collide with each other. Thus, we suggest that massive satellites as the Galilean ones and close-in super-Earths might be formed through similar processes.

In our first set of models, the disc surface density has a strong radial dependence ( $\Sigma_{\text{gas}} \propto r^{-3/2}$ ) and the aspect ratio of the disc was  $h = 0.05$ . As a consequence, the embryos in the outer disc grow slower than the inner ones, the migration speed of them is slow, and in most of the cases these bodies never reach the inner region where the Jovian satellites are located. On the other hand, When a uniform distribution for the gaseous disc was used, we found that the outer embryos migrated faster and interacted with the inner ones. In this way, the final radial distribution of satellites was improved showing better agreement with the observations. Our results indicate that flatter density distributions with a weak radial dependence favour the migration of satellite embryos from the outer disc. However, the final masses of the satellites remained an issue. As in the previous cases, the massive satellites tend to reach the inner cavity of the disc and, due to interactions with other satellites, eventually fall into the planet. Szulágyi et al. (2016) performed detailed hydrodynamic studies about circum-planetary discs around giant planets and showed that the gaseous disc is flatter in the region of the Galilean satellites corroborating our findings.

The temperature distribution in the disc is an important feature to study the evolution of satellites in a circum-planetary disc. In our first models, we adopted the aspect ratio to be  $h = 0.05$ , which is a generally good estimate for  $h$  in protoplanetary discs. However, in

our model for Jupiter's circum-planetary disc, this value implies a disc with an ice line very close to the central planet (around  $4R_J$ ), which is in disagreement with the values found in the literature. A well accepted position for the ice line in models like ours is at  $30R_J$  (Lunine & Stevenson 1982; Miguel & Ida 2016). As the initial temperature depends on the aspect ratio (equation 18) we adopted in a second sequence of models  $h = 0.15$ . Increasing the value of the aspect ratio also has implications on the migration of the embryos; once they are evolving in a thicker disc, it is expected that their migration rate decrease. Our simulations showed that this configuration of the disc favours the formation of massive satellites,  $M \geq 6 \times 10^{-5} M_J$ , which is comparable to the masses of Ganymede and Callisto. We highlight the results from model `multi-sat-uni-1-h015`, where four satellites were formed with masses that accurately match the masses of the Galilean satellites.

Reproducing the formation and evolution of the Galilean satellites is not a simple task, the processes that led to the formation of these bodies are complicated and full of uncertainties. With this paper, we expect to combine results of our simulations to add informations about the origin of the embryos that gave birth to this satellite system; also, we found that a flatter initial gas distribution and a disc with ice line around  $30R_J$  favour the formation of systems like the Jovian system. We suggest that the similarities between the Galilean satellite system and the close-in super-Earth system might lead to a unified theory about the formation of these systems.

## ACKNOWLEDGEMENTS

We thank the anonymous referee for the valuable comments and suggestions. We thank Andre Izidoro for the discussions concerning our findings during the participation in the 'Protoplanetary Disks and Planet Formation and Evolution' programme organized by the Munich Institute for Astro-and Particle Physics (MIAPP). R.A.M. thanks financial support from Fundação de Amparo à Pesquisa do Estado de São Paulo (Grants: 2011/08171-3, 2013/24281-9 and 2016/12113-2).

## REFERENCES

- Adachi I., Hayashi C., Nakazawa K., 1976, *Prog. Theor. Phys.*, 56, 1756
- Brasser R., Duncan M. J., Levison H. F., 2007, *Icarus*, 191, 413
- Canup R. M., Ward W. R., 2002, *AJ*, 124, 3404
- Canup R. M., Ward W. R., 2006, *Nature*, 441, 834
- Canup R. M., Ward W. R., 2009, *Origin of Europa and the Galilean Satellites*. University of Arizona Press, Tucson, p. 59
- Chambers J. E., 1999, *MNRAS*, 304, 793
- Cresswell P., Nelson R. P., 2008, *A&A*, 482, 677
- Estrada P. R., Mosqueira I., Lissauer J. J., D'Angelo G., Cruikshank D. P., 2009, *Formation of Jupiter and Conditions for Accretion of the Galilean Satellites*. University of Arizona Press, Tucson, p. 27
- Fujii Y. I., Okuzumi S., Tanigawa T., Inutsuka S.-i., 2014, *ApJ*, 785, 101
- Fujii Y. I., Kobayashi H., Takahashi S. Z., Gressel O., 2017, *AJ*, 153, 194
- Gillon M. et al., 2016, *Nature*, 533, 221
- Gillon M. et al., 2017, *Nature*, 542, 456
- Greenberg R., 1987, *Icarus*, 70, 334
- Hayashi C., 1981, *Prog. Theor. Phys. Suppl.*, 70, 35
- Heller R., Pudritz R., 2015a, *A&A*, 578, A19
- Heller R., Pudritz R., 2015b, *ApJ*, 806, 181
- Howard A. W. et al., 2012, *ApJS*, 201, 15
- Ida S., Lin D. N. C., 2004, *ApJ*, 616, 567
- Izidoro A., Morbidelli A., Raymond S. N., 2014, *ApJ*, 794, 11
- Izidoro A., Raymond S. N., Pierens A., Morbidelli A., Winter O. C., Nesvorný D., 2016, *ApJ*, 833, 40

- Izidoro A., Ogihara M., Raymond S. N., Morbidelli A., Pierens A., Bitsch B., Cossou C., Hersant F., 2017, *MNRAS*, 470, 1750
- Kley W., 1999, *MNRAS*, 303, 696
- Kokubo E., Ida S., 2002, *ApJ*, 581, 666
- Lubow S. H., Seibert M., Artymowicz P., 1999, *ApJ*, 526, 1001
- Luger R. et al., 2017, *Nature Astron.*, 1, 0129
- Lunine J. I., Stevenson D. J., 1982, *Icarus*, 52, 14
- Masset F., 2000, *A&A*, 141, 165
- Mayor M. et al., 2011, *A&A*, preprint ([arXiv:1109.2497](https://arxiv.org/abs/1109.2497))
- Miguel Y., Ida S., 2016, *Icarus*, 266, 1
- Mosqueira I., Estrada P. R., 2003a, *Icarus*, 163, 198
- Mosqueira I., Estrada P. R., 2003b, *Icarus*, 163, 232
- Ogihara M., Ida S., 2012, *ApJ*, 753, 60
- Ormel C. W., Liu B., Schoonenberg D., 2017, *A&A*, 604, A1
- Papaloizou J. C. B., Larwood J. D., 2000, *MNRAS*, 315, 823
- Peale S. J., Lee M. H., 2002, *Science*, 298, 593
- Petigura E. A., Howard A. W., Marcy G. W., 2013, *Proc. Natl. Acad. Sci.*, 110, 19273
- Raymond S. N., Quinn T., Lunine J. I., 2005, *ApJ*, 632, 670
- Sasaki T., Stewart G. R., Ida S., 2010, *ApJ*, 714, 1052
- Shakura N. I., Sunyaev R. A., 1973, *A&A*, 24, 337
- Stoll M. H. R., Kley W., 2014, *A&A*, 572, A77
- Stoll M. H. R., Kley W., Picogna G., 2017a, *A&A*, 599, L6
- Stoll M. H. R., Picogna G., Kley W., 2017b, *A&A*, 604, A28
- Szulágyi J., Masset F., Lega E., Crida A., Morbidelli A., Guillot T., 2016, *MNRAS*, 460, 2853
- Takata T., Stevenson D. J., 1996, *Icarus*, 123, 404
- Tanaka H., Ward W. R., 2004, *ApJ*, 602, 388
- Tanigawa T., Ohtsuki K., Machida M. N., 2012, *ApJ*, 747, 47
- Turner N. J., Lee M. H., Sano T., 2014, *ApJ*, 783, 14
- Weidenschilling S. J., 1977, *MNRAS*, 180, 57
- Yoder C. F., 1979, *Nature*, 279, 767
- Yoder C. F., Peale S. J., 1981, *Icarus*, 47, 1

This paper has been typeset from a  $\text{\LaTeX}$  file prepared by the author.